Article

Chitin and Silk Fibroin Biopolymers Modified by Oxone: Efficient Heterogeneous Catalysts for Knoevenagel Reaction

Fernando B. Neves [1], Lucas L. Zanin [2], Rayanne R. Pereira [1,3], José Otávio C. S. Júnior [3], Roseane Maria R. Costa [3], André L. M. Porto [2], Sérgio A. Yoshioka [4], Alex Nazaré de Oliveira [1], David E. Q. Jimenez [1,*] and Irlon M. Ferreira [1,*]

[1] Applied Organic Synthesis and Biocatalysis Laboratory, Chemistry Course, Federal University of Amapá, Marco Zero University Campus of Ecuador, KM–02 Bairro Zerão, Macapá 68902-280, AP, Brazil
[2] Organic Chemistry and Biocatalysis Laboratory, São Carlos Institute of Chemistry, University of São Paulo, Av. John Dagnone, 1100, Ed. Environmental Chemistry, Santa Angelina, São Carlos 13563-120, SP, Brazil
[3] Cosmetic Laboratory, Faculty of Pharmaceutical Sciences, Federal University of Pará, Belém 66075–110, PA, Brazil
[4] Biochemistry and Biomaterials Laboratory, Institute of Chemistry of São Carlos, University of São Paulo, Av. Trabalhador São-Carlense, 400, São Carlos 13560-970, SP, Brazil
* Correspondence: derteriom@unifap.br (D.E.Q.J.); irlon.ferreira@unifap.br (I.M.F.)

Abstract: New materials from silk fibroin (FS-Ox) and chitin (CT-Ox) functionalized with Oxone® salt were developed for application in the synthesis of Knoevenagel adducts. The experiments were performed using benzaldehyde derivatives, malononitrile, and a mixture of water and ethanol as green solvents. The efficiency of conventional and microwave irradiation as heating sources for this reaction was also investigated. When the reactions were performed for 60 min under optimized conditions with conventional heating, twelve Knoevenagel adducts **2a–l** were obtained, with good yields for both catalysts (CT-Ox 60–98% and FS-Ox 71–98%). When microwave irradiation was used, the reaction periods were reduced twelvefold, with the same Knoevenagel adducts with good CT-Ox (39–99%) and FS-Ox (35–99%) yields obtained in most cases. The reuse of these materials as catalysts in successive reactions was also evaluated, and CT-Ox FS-Ox were successfully used for 4 and 2 cycles, respectively. The results presented prove the efficiency of the CT-OxFS-Ox catalyst as a promising low-cost and reusable material with suitable catalytic properties to be applied in the aldol condensation reaction in a sustainable way.

1. Introduction

Organic synthesis is an important field development of new compounds, especially in the case of molecules with biological activity. One example is Knoevenagel condensation, which can provide new C-C bonds via the reaction between aldehydes or ketones and methylene compounds containing acidic hydrogens [1–4]. Many studies of Knoevenagel adducts have tested new reaction conditions, such as catalyst-free, polymer-basic materials, focusing on green chemistry [5–8].

One of the biopolymers used in the organic reactions as support [9] or a catalyst [10,11] is silk fibroin, a natural macromolecular protein with a block copolymer structure formed of large hydrophobic domains and small hydrophilic spacers. It has strong mechanical properties, is a versatile material for biotechnology processes, and contains accessible functional groups for chemical modifications, making it favorable for the development of new biocatalysts or supports [2,9–11].

Jimenez et al. [1] reported Knoevenagel synthesis with benzaldehyde derivatives and malononitrile using fibroin functionalized with $CuSO_4$ as catalyst, using microwave irradiation as a heating source. The reactions were performed at 60 °C for 30 min, and

adducts with excellent yields of 97–99% were obtained. Kuhbeck et al. [12] researched the C-C bond formation using fibroin as a green catalyst. The material was applied in a Knoevenagel condensation reaction from 2-nitrobenzaldehyde, and adducts with 84% yield were obtained. In addition, this biodegradable material performed well when used in other reactions, such as Henry and Michael additions [4,12,13].

Chitin is a linear polysaccharide containing *N*-acetyl-d-glucosamine repeating units connected through β-(1-4)-glycosidic linkages [13,14]. This biopolymer is widely extracted from a number of living organisms, such as shrimps [14,15], and has attracted growing interest in the field of catalysis [16,17]. The presence of amine and hydroxyl groups provides a large scope of potentially useful applications for chitin or chitosan, as they can be modified to improve certain properties of this biopolymer. Chitosan has been used as an efficient heterogeneous organocatalyst, demonstrating an ability to bind with several transition metal ions, making it an attractive solid support for the preparation of several reactions such as Knoevenagel, esterification, and Michael addition [3,4,13,16,18,19].

Anbu and coworkers [20] reported Knoevenagel condensation reactions with aromatic aldehydes and malonic acid, using DMF as a solvent and chitosan as a catalyst. This methodology provided fifteen adducts with 25–98% yields. Rani et al. [16] described the use of chitosan as a catalyst for aldol reactions in a water medium. The experiments were performed with aromatic aldehydes, ethyl acetoacetate, or dimethylmalonate, and eleven Knoevenagel products were synthesized with 13–90% yields. Sakthivel et al. [3] also studied the use of chitosan in this reaction type. Using ethanol as a solvent, ten Knoevenagel adducts were obtained with moderate to good yields of 53–99%.

The present study focused on the development of natural materials, such as fibroin and chitin modified with Oxone®, applied in a Knoevenagel condensation reaction, in accordance with green chemistry protocols. The new functionalized catalysts reduced reaction time, increased adduct yields, and could be reused.
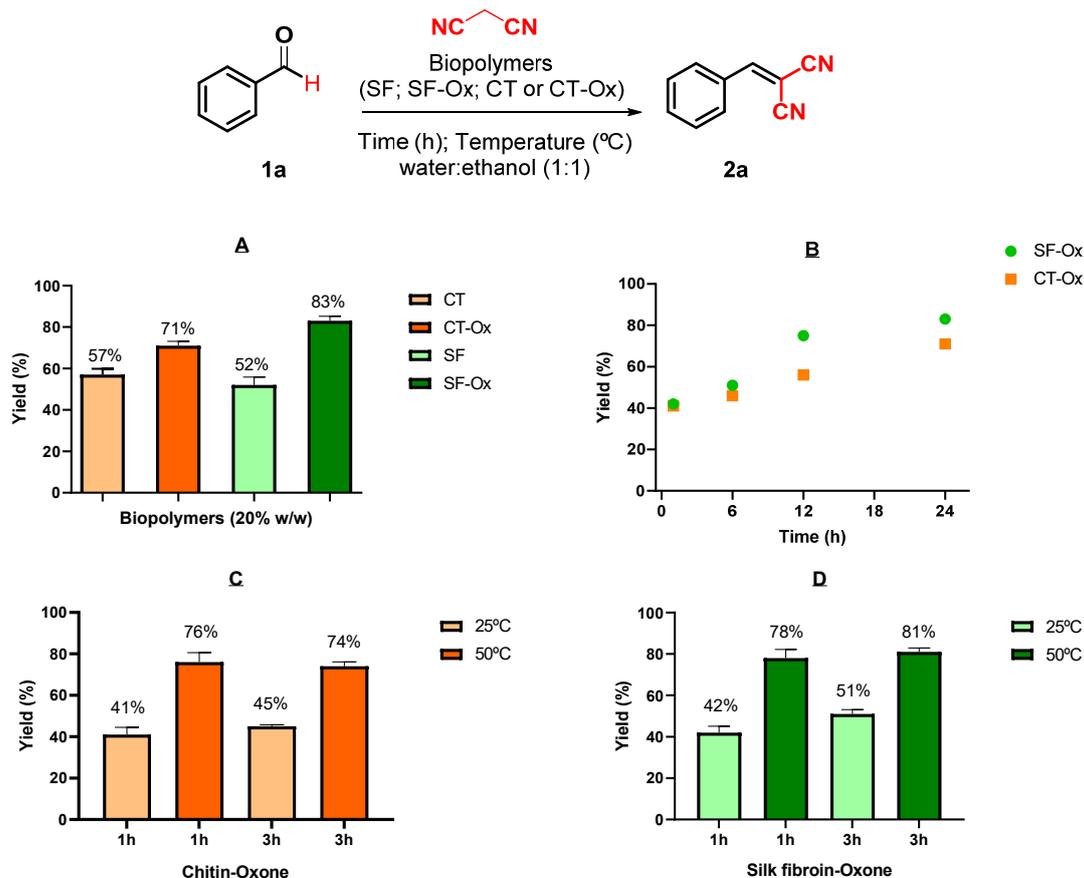
2. Results and Discussion

2.1. The Use of Modified Biopolymers as Catalysts in a Knoevenagel Reaction under Conventional Heating

Initially, the natural forms of SF and CT were evaluated as heterogeneous organocatalysts for the Knoevenagel reaction. The reaction between benzaldehyde **1a**, malononitrile, and a water/ethanol mixture (1:1) as a solvent was used as a model. Two experiments were performed under room temperature conditions for 24 h, and the 2-benzylidenemalononitrile **2a** was obtained with yields of 52% and 57% for SF and CT, respectively. When the reaction was performed with modified biopolymers, the adduct **2a** obtained had better yields of 83% and 71% for SF-Ox and CT-Ox, respectively (Figure 1A). This result showed that the modified biopolymers, SF-Ox and CT-Ox, acted as catalysts in the Knoevenagel reaction, and that they were more efficient in this process than the biopolymers in their natural form (SF and CT). Therefore, new reaction conditions employing CT-Ox and FS-Ox were investigated.

Different reaction times (1, 6, 12, and 24 h) were evaluated at room temperature (Figure 1B). In the first hour of reaction, both biopolymers demonstrated effectiveness in the formation of **2a**, with yields of 42% and 41%, respectively, for SF-Ox and CT-Ox. After 12 h of reaction, the yield of **2a** increased to 56% with the use of CT-Ox. These results showed that the reaction yield with CT-Ox remained practically unchanged during the first 12 h of reaction. However, the reaction yield with SF-Ox after 12 h was 75%, showing that this biomaterial was more efficient in the formation of adduct **2a**.

In the next optimization step, the effect of temperature on the reaction progress was evaluated. The experiments were performed at 50 °C and monitored during a 1 h to 3 h period. The condensation reaction in the presence of CT-Ox provided a good yield (76%) at 50 °C after 1 h, with a similar yield obtained when the reaction was performed for 3 h (Figure 1C). When SF-Ox was used, after 1 h of reaction adduct **2a** was obtained with a yield of 78%. At 3 h, a slight increase was observed and adduct **2a** was obtained with a yield of 81% (Figure 1D).
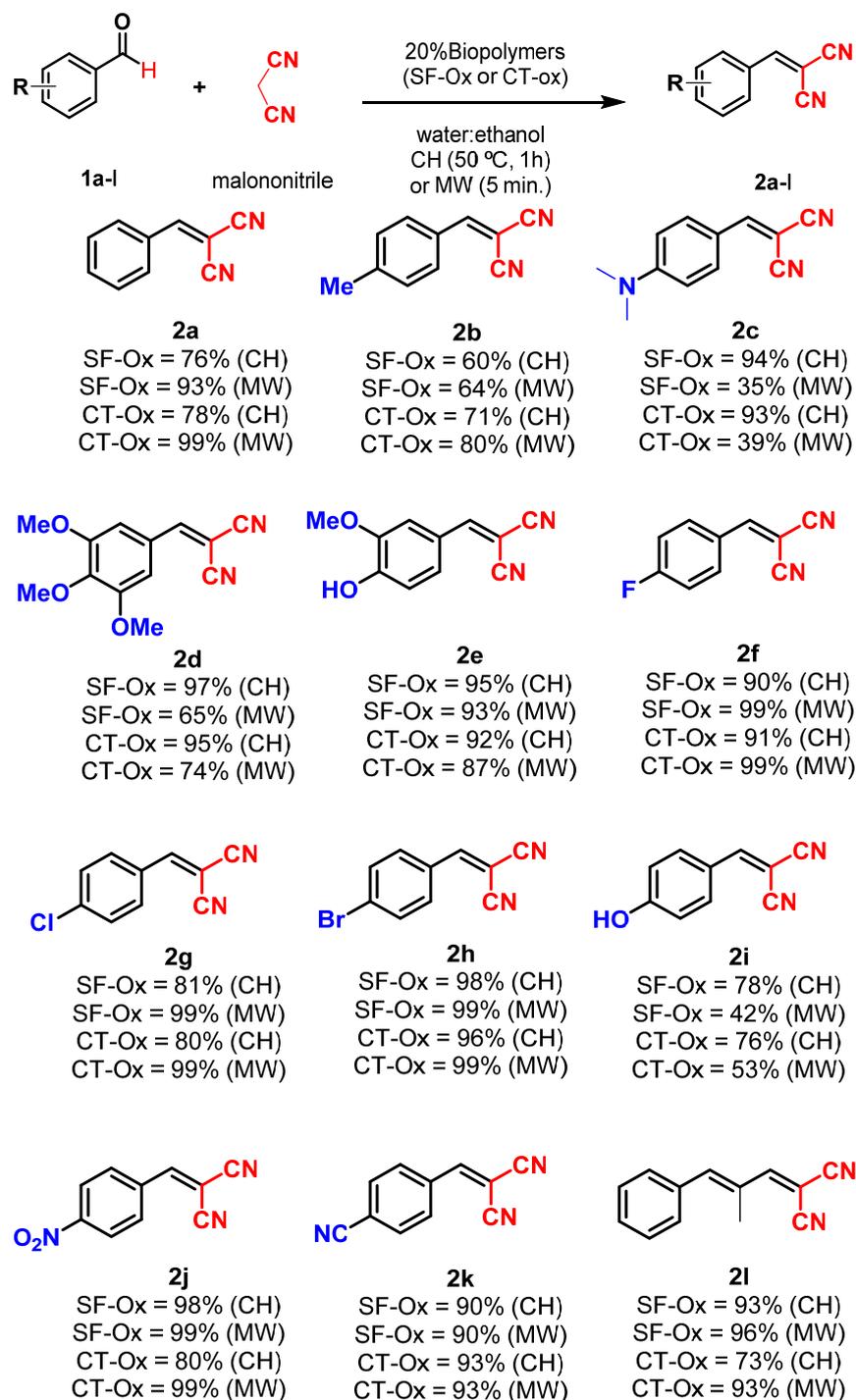
Figure 1. Optimization of Knoevenagel condensation reaction using aldehyde **1a** (2 mmol) and malononitrile (2.5 mmol) with and without biopolymers (20% *w/w*) as catalysts. (**A**) Screening of biopolymers (rt and 24 h); (**B**) effect of time [1, 3, 6, 12 and 24 h (r.t.)] in presence of CT-Ox and SF-Ox; (**C**) effect of temperature (25 or 50 °C for 1 or 3 h) with CT-Ox; (**D**) effect of temperature (25 or 50 °C at 1 or 3 h) with SF-Ox.

An important parameter optimized in the reaction using immobilized biopolymers was catalyst loading. To achieve this, three different amounts (10, 20, and 30% *w/w*) of SF-Ox and CT-Ox were tested (Figure 2). The data confirmed a gradual increase in **2a** yield in accordance with the mass of immobilized biopolymer used. The best results were observed with 30% *w/w* of both biopolymers, yielding 99% (SF-Ox) and >99% (CT-Ox) for adduct **2a**, respectively. However, as good yields had already been obtained with 20% of the biocatalysts, this amount was selected for the rest of the study.

Next, the optimized conditions (20% of catalysts, at 50 °C, for 1 h) were applied in reactions with different aldehydes **1a–l** and malononitrile to identify the scope of the Knoevenagel adducts (Figure 2). The adducts **2a–l** were obtained with good to excellent yields (60–98%). All compounds were characterized by NMR, FT-IR spectra, melting point, and GC-MS analysis.

When aldehydes, with electron-donating groups, were used (**2b–e**), reaction with biopolymers (FS-Ox or CT-Ox) exhibited good yields (60–97%). Therefore, the success of the reaction does not depend on the electronic effects promoted by the substituent attached to the aromatic ring. The compound **2b** was isolated with a yield of 60% and 71%, for FS-Ox and CT-Ox, respectively. Reactions in the presence of SF-Ox provided the higher yields of the products **2c**, **2d**, and **2e**, with 94%, 97%, and 95%, respectively. Similar results were obtained with CT-Ox, with the adducts **2c**, **2d**, and **2e** obtained with good yields, 93%, 95%, and 92%, respectively (Figure 2).

Figure 2. Knoevenagel condensation synthesis using aromatic aldehyde derivatives, malononitrile and immobilized biopolymers with Oxone® as catalysts under conventional heating (CH) or with microwave irradiation (MW) as a heating source.

Aldehydes with different halogenate substituents resulted in excellent yields for 2-(4-fluorobenzylidene)malononitrile (**2f**), 2-(4-chlorobenzy-lidene)malononitrile (**2g**), and 2-(4-bromobenzylidene)malononitrile (**2h**) with both biopolymers [90, 81 and 98%, respectively, for FS-Ox, and 91%, 80%, and 96%, respectively, for CT-Ox] (Figure 2).

A similar range of good yields was obtained with electron withdrawing groups. The products **2i**, **2j**, and **2k** were obtained at yields of 78%, 98%, and 90%, respectively, for SF-Ox, and 73%, 95%, and 93%, respectively, for CT-Ox (Figure 2) (Supplementary Materials).

2.2. The Use of Modified Biopolymers as Catalysts in the Knoevenagel Reaction Using Microwave Irradiation as a Heating Source

Microwave (MW) chemistry was the subject of the second part of this study. In order to achieve even better performances with the supported biopolymers and this type of heating source, a new synthetic optimization process was performed, again involving the synthesis of adduct **2a** as a reaction model, and the same temperature used as in conventional heating conditions (50 °C).

In the first attempt, employing CT-Ox, the reaction was performed for 60 min. After GC-MS analysis, adduct **2a** was obtained with a yield of 99% (entry 1, Table 1). This result already represents an advance, as in the same reaction period, under conventional heating, compound **2a** was obtained at a lower yield of 78%.

Table 1. Optimization process for the synthesis of Knoevenagel adduct **2a** using CT-Ox or FS-Ox as a catalyst under MW irradiation as a heating source.

Entry	Heat Source	Catalyst	Temp. (°C)	Time (min)	Conversion [b] (%)	Isolated Yield (%)
1	MW	CT-Ox [a]	50	60	99	—
2	MW	CT-Ox [a]	50	10	97	—
3	**MW**	**CT-Ox [a]**	**50**	**5**	**95**	**89**
4	MW	SF-Ox [a]	50	5	62	56
5	MW	—	50	5	45	40

Reaction conditions: 1 mmol of aldehyde; 1.25 mmol of malononitrile; 4 mL of solvent mixture (H_2O-EtOH); Temp. = temperature; [a] = 20 mol%; [b] = conversion calculated by GC-MS analysis (Supplementary Materials).

In the following experiments, the reaction time was reduced to verify the efficiency of the biomaterial in faster reactions. When the synthesis of **2a** was performed for 10 min, the conversion remained high (97%, entry 2, Table 1). When the reaction was carried out in 5 min, the conversion of **2a** also remained high (95%), as did the isolated yield value of adduct **2a** (89%, entry 3, Table 1). This is a significant result as the reaction efficiency was reduced twelvefold in relation to the methodology involving conventional heating (CT-Ox, 78% for **2a**, in 1h under CH; Ct-OX, 89% for **2a**, in 5 min. under MW).

The same reaction conditions (entry 3, Table 1) were applied when using the biomaterial SF-Ox for the synthesis of adduct **2a**. In this case, the conversion obtained was moderate (62%); however, the extremely short reaction time in which the synthesis was carried out should be noted (entry 4, Table 1).

Finally, the synthesis of **2a** was performed in absence of catalyst. The results showed that the presence of supported biopolymers influenced the reaction progress, as a conversion of only 45% for **2a** was obtained when the reaction was carried out without any such materials (entry 5, Table 1).

After the reaction optimization in MW reactor, the scope of Knoevenagel adducts was again analyzed. The adducts **2a–i** were obtained with moderate to excellent yields (35–99%, Figure 2). In this step, the lowest yield values were obtained for the adducts **2c** and **2i**. These compounds have strong activating groups [$(CH_3)_2$N-Ar and OH-Ar] in their precursor aldehydes, attached to their aromatic rings. It is believed that, as the reactions were carried out over a short period (5 min under MW conditions), the electronic effects had consequences on the reaction yield, explaining the low values. In comparison, in the

first stage of the study, it was likely that the reaction times of 1h were long enough for the electronic effects to not have significant consequences on product yields.

2.3. Reuse of the Biopolymers Fs-Ox and CT-Ox in the Knoevenagel Condensation Reactions

One of the advantages of heterogeneous catalysts in comparison with homogeneous catalysts is their capacity for reuse, which can help to reduce operating costs [3]. In this stage of the study, the reusability of the support biopolymers SF-Ox and CT-Ox in the Knoevenagel reaction was evaluated. Moreover, the effectiveness of both CH and MW as heating sources was assessed.

2.3.1. Reuse of SF-Ox and CT-Ox under CH Conditions in the Synthesis of Adduct **2a**

Employing SF-Ox under CH conditions, adduct **2a** was obtained at a 75% yield in the first cycle. At the end of the reaction, the content was filtered and washed with 25 mL of EtOAc. The catalyst, retained on the filter, was then dried in an oven (85 °C), and reused successively. The yields for the second and the third cycle were 74 and 68%, respectively.

During the reuse of CT-Ox, the yield of **2a** decreased significantly. On first use, a yield of 76% of **2a** was obtained, while on second use the yield fell to 50% and to 38% on the third use (Table 2).

Table 2. Reuse of SF-Ox and CT-Ox in the formation reaction of adduct **2a**.

Biopolymers	Conversion (%)		
	Cycle 1	Cycle 2	Cycle 3
SF-Ox [a]	75	74	68
SF-Ox [b]	99	99	—
CT-Ox [a]	76	50	38
CT-Ox [b]	99	99	99

[a] conventional heating as heating source used for the synthesis of 2a; [b] microwave irradiation as heating source used for the synthesis of 2 h.

2.3.2. Reuse of SF-Ox and CT-Ox under MW Conditions in the Synthesis of Adduct **2a**

The reuse of both biomaterials was also evaluated with MW heating conditions. For this, the synthesis of adduct **2h** was selected as a model.

The performance of CT-Ox with MW as a heating source was better than under CH conditions. The yields of adduct **2h** for the first, second, and third reuse were >99%, demonstrating that the material did not lose its catalytic efficiency even when reused three times (Table 2). However, catalyst mass was lost during the recovery steps, making it impossible to recover a sufficient mass for a fourth reaction cycle.

As with the CT-Ox biopolymer, when using SF-Ox with MW as a heating source, a high catalytic efficiency was observed, with the product **2h** obtained at a 99% yield with a fresh use of this biocatalyst. However, this material exhibited low recovery capacity, and due to the high mass loss, could only be used once more. Interestingly, the catalytic efficiency did not change and the adduct **2h** was again obtained at a 99% yield (Table 2). It can therefore be seen that this biomaterial does not undergo changes in its catalytic sites, which are fundamental for the progress of the reaction. Due to its extremely sensitive and brittle morphology, however, the system becomes practically homogeneous at the end of the reaction, making recovery difficult.
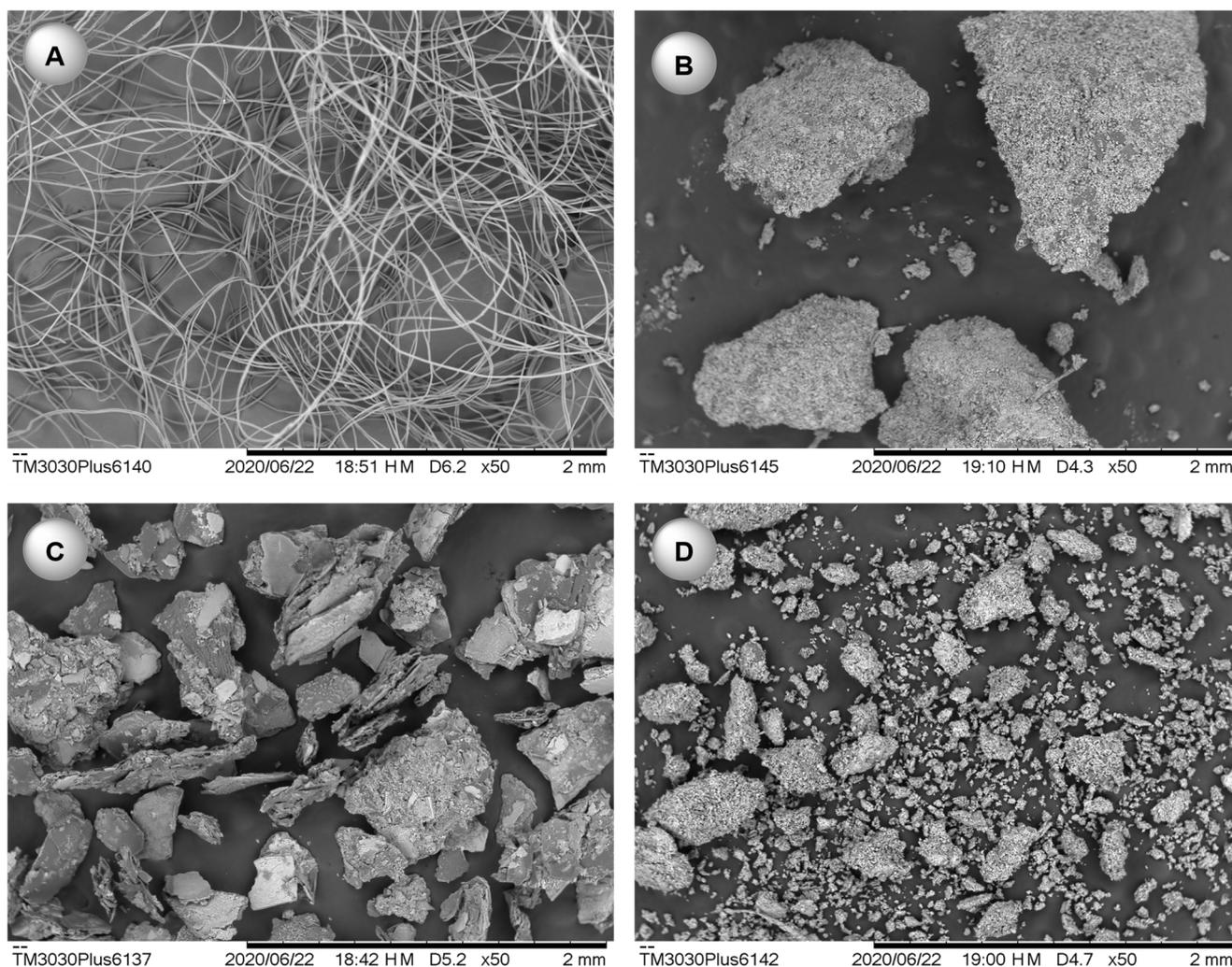
From the results obtained, it was observed that the catalytic efficiencies of CT-Ox and SF-Ox do not change when these biopolymers are submitted to heating via MW. The reuse of both is limited by the loss of mass during the recovery process.

2.4. Characterization of the New Fs-Ox and CT-Ox Materials Used in Knoevenagel Condensation

The triple salt potassium peroxymonosulfate ($2KHSO_5 \cdot KHSO_4 \cdot K_2SO_4$) known as Oxone® is an effective oxidant agent. Oxone® salt was used to obtain spherical crystalline chitin nanoparticles [21] and silk microfibers [9–11], and represents an easy and eco-friendly

procedure because of its stability and water solubility, its low cost, its less toxic 'green' nature, its non-polluting by-products, and its cost-effectiveness [2,10,12,21–23].

The traditional method for generating SF is a ternary solution of $CaCl_2$:EtOH:H_2O. When silk cocoons are treated through the traditional method using Na_2CO_3 (2%), the main morphological characteristics of SF are its elongated smooth fibers, as seen in Figure 3A. In contrast, fiber morphology and size were significantly influenced by treatment with Oxone® (Figure 3B). These results suggested that Oxone® salt in the presence of Ca^{2+} ions acts as a mineralizing agent in the peptide bonds present in silk fibroin, increasing the contact surface of the biocatalytic FS-Ox [10].
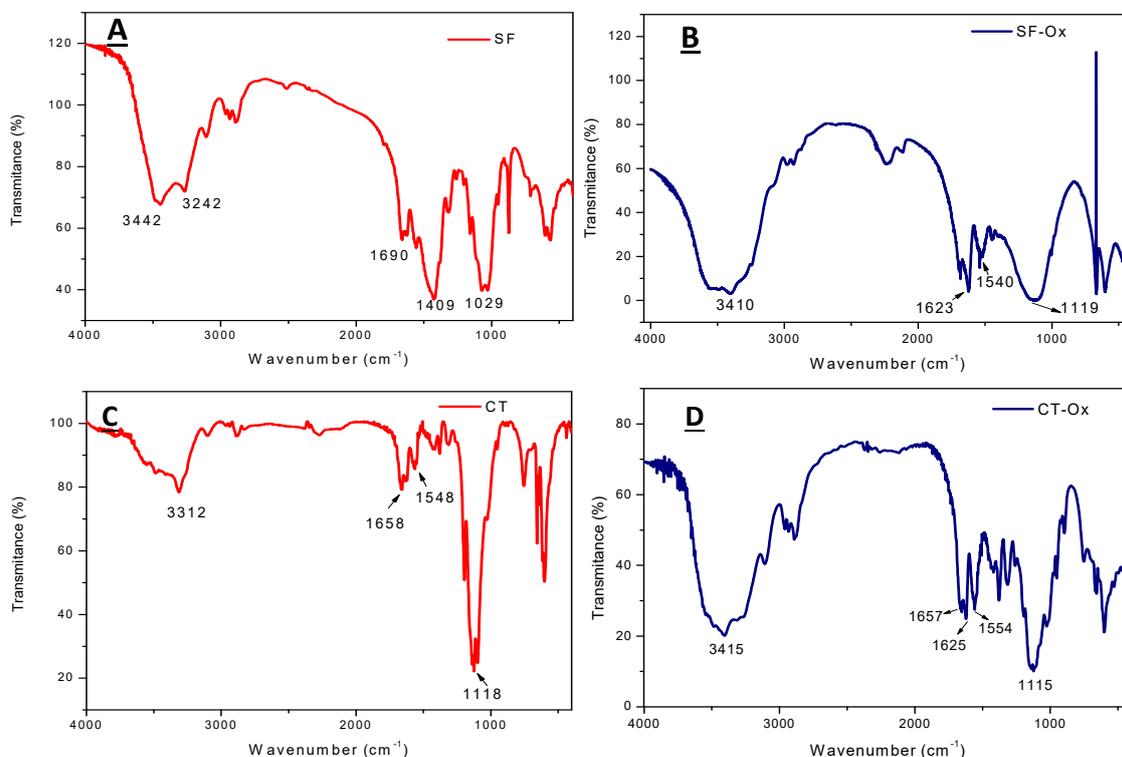

Figure 3. Scanning electron microscopy images of silk-fibroin (**A**), silk-fibroin-Oxone® (**B**), chitin (**C**), and chitin-Oxone® (**D**).

The common chemical process for the modification of chitin involves the use of harsh chemicals (acid and alkali solutions) under elevated temperatures for a prolonged incubation period [13,24]. The active potassium peroxymonosulfate ($KHSO_5$) first attacked the terminal glucosidic bond of the chitin chain to loosen up the crystallites to allow penetration by water and Oxone®. Like acids, $KHSO_5$ was capable of hydrolyzing the β-(1-4) bonds, with the presence of water then rendering each broken bond inactive. Oxone® was effective in the cleavage of the glycosidic bonds and etching out the individualization of the elementary fibrils for CT-Ox [21].

The FTIR spectra of FS and FS-Ox (Figure 4A,B) exhibited a characteristic sharp, intense peak at 3609 cm^{-1}, belonging to the N-H group of stretching vibrations, and another peak

at 3451 cm^{-1}, possibly due to the vibration of the O-H groups of phenols from tyrosine and serine. Peaks associated with the N-H group from peptides and asymmetrical stretching of the C-H bonds were also detected at 3364 cm^{-1} and 2931 cm^{-1}, respectively [25]. Positively charged calcium ions interact with the negatively charged carbonyl groups from fibroin, which can be verified by the intensity levels [26].
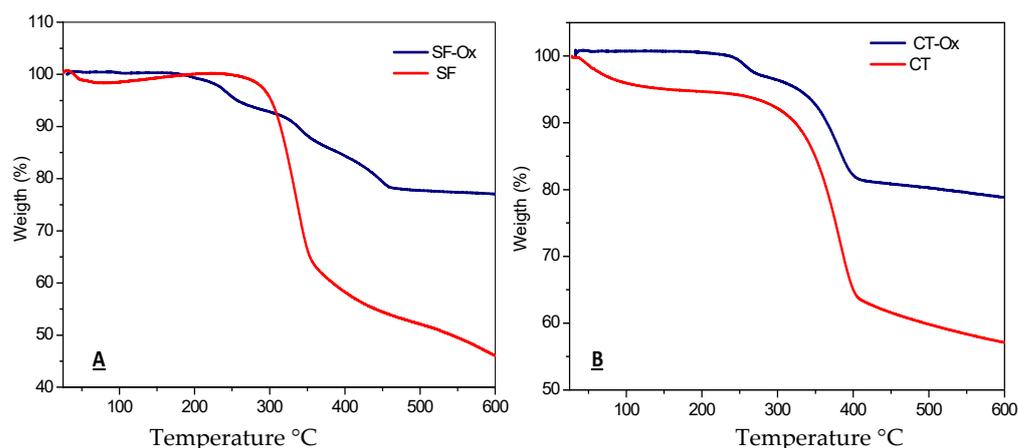

Figure 4. FTIR spectra of silk-fibroin (**A**) and silk-fibroin-Oxone® (**B**); chitin (**C**) and chitin-Oxone® (**D**).

The FT-IR spectra of CT and CT-Ox are shown in Figure 4C,D. The two bands around 1658 cm^{-1} for CT and 1657 cm^{-1} for CT-Ox confirm the presence of an amide group. For CT, however, the broad band around 3312 cm^{-1} is related to the axial stretching of a single bond O-H group, which appears superimposed on the N-H single bond stretching band. For CT-Ox, meanwhile, there was a shift to 3415 cm^{-1}, resulting from the treatment with Oxone®. The peak for the asymmetric stretching of C-O-C was observed at 1115–1118 cm^{-1} in both cases [27–29].

The thermal behavior of the pure SF and SF-Ox was analyzed by thermogravimetric analysis (TGA). The degradation temperature, known to be a criterion of thermal degr1adation, was calculated based on differential TGA curves (Figure 5). The fibroin TG curve showed a single mass loss step at a temperature of 266.6 °C. From this point (266.66 °C), the fibroin TG curve descends, implying a progressive loss of mass until the end of the analysis at 600 °C. The thermal decomposition of fibroin is related to the breakdown of side chain groups of amino acid residues, as well as the cleavage of the peptide bonds [30]. In addition, the thermal decomposition of fibroin at temperatures above 300 °C is associated with the thermal degradation of silk fibroin with a β-sheet structure oriented along the fiber [11].

The chitin TG curve exhibited a mass loss of 32.124% in the range of 243–422 °C (Figure 5B). The thermal decomposition of chitin is related to the depolymerization/decomposition of polymeric chains through deacetylation and the cleavage of the glycosidic bonds, in addition to the destruction of the pyranose ring [15].

Figure 5. Thermogravimetric analysis of the biopolymers SF-Ox and SF (**A**); CT-Ox and CT-Ox (**B**).

Figures 4B and 5A show the TG curves of fibroin and chitin after treatment with Oxone® salt. In both curves, it can be seen that the polymers present greater thermal stability after treatment with Oxone®. SF-Ox presents a mass loss range of between 288.15 °C and 432.5 °C, with a 20% mass loss, while CT-Ox presents a mass loss range of between 166.96 °C and 485 °C, with 23% mass loss. SF-Ox exhibits a residue of 80%, and CT-Ox exhibits a residue of 77%, with a larger residue signifying a greater resistance to thermal decomposition, as is the case with CT-Ox and SF-Ox, depending on the mineralization provided by Oxone® [10].

3. Materials and Methods

3.1. Chemical, Reagents and Catalysts

Cocoons of the silkworm (*Bombyx mori*) were kindly provided by Prof. Dr. Sérgio A. Yoshioka (São Carlos, São Paulo, Brazil). Oxone® ($KHSO_5 \cdot 0.5KHSO_4 \cdot 0.5K_2SO_4$) was purchased from Sigma-Aldrich (São Paulo, Brazil). $CaCl_2.2H_2O$ (99%) and $NaCO_3$ (99%) were purchased from Vetec. Ethanol (EtOH, 99.5%) was purchased from Synth (São Paulo, State of São Paulo, Brazil). Benzaldehyde **1a** (99.5%), 4-methoxybenzaldehyde 1b (98%), 4-(dimethylamino)benzaldehyde 1c (98%), 3,4,5-trimethoxybenzaldehyde 1d (99%), 4-hydroxy-3-methoxybenzaldehyde 1e (98%), 4-fluorobenzaldehyde 1f (98%), 4-chlorobenzaldehyde 1g (97%), 4-bromobenzaldehyde 1h (99%),4-hydroxybenzaldehyde 1i (98%), 4-nitrobenzaldehyde 1j (98%), 4-formylbenzonitrile 1k (95%), cinnamaldehyde 1l (98%), and malononitrile (99%) were purchased from Sigma-Aldrich (São Paulo, State of São Paulo, Brazil). and were used without further purification.

Ethyl acetate (EtOAc), hexane, and sodium sulfate were purchased from different suppliers (Aldrich, Fluka, Synth, Merck, and Vertec). The deuterated solvents, acetone-d_6 (99.8%), DMSO-d_6 (99.9%), and $CDCl_3$ (99.8%) were purchased from Cambridge Isotope Laboratories (Scielab, Rio de Janeiro, RJ, Brazil).

The thin-layer chromatography (TLC) utilized was DC-Fertigfolien ALUGRAM® XTra SIL G/UV$_{254}$ (layer: 0.20 mm silica 60 with fluorescent indicator UV$_{254}$) (São Carlos Química, São Carlos, SP, Brazil). In all cases, analysis was performed using a mixture of hexane and ethyl acetate (8:2).

Purifications in a chromatography column were performed using silica gel (technical grade, pore size 60 A, 230–400 mesh particle size, 40–63 μm particle size) as the stationary phase. This was purchased from Sigma-Aldrich (São Paulo, State of São Paulo, Brazil).

3.2. Preparing the Silk Fibroin (SF)

The silk fibroin (SF) solution was prepared from the perforated silkworm cocoon material (3.0 g). The SF was then transferred to a 2% Na_2CO_3 solution (500 mL), to be heated to a temperature of 80 °C and stirred magnetically for 30 min. This provided the fibrous material. Lastly, the fibers were washed with distilled water (3 × 500 mL) and dried

in an oven (70 °C; 24 h). Details of the protocol for preparing the fibers from the cocoon were described in the literature [9–11].

3.3. Modification of Silk Fiber by Oxone (SF-Oxone®)

The modification of the silk fiber by Oxone® was carried out in a Becker flask (50 mL), in which 0.5 g of SF was added to 50 mL of EtOH with 0.5 g of Oxone®. The mixture was magnetically stirred for 3 h at 50 °C. The material was then washed with distilled water and dried in an oven (70 °C, 24 h).

3.4. Obtaining and Preparing the Chitin

Chitin was isolated from the shrimp exoskeleton abdominal residue, following the protocol described [13,14,31].

(a) *Selection and pre-treatment of samples*: Selection, washing, drying, and grinding of residues were carried out. The exoskeleton (abdomen region) was manually selected and washed with water to remove impurities. After this process, the biomaterial was dried in an oven (50 °C) for 24 h. After this period, the material was crushed in an industrial blender and particle size separation was performed in a 200-mesh sieve.

(b) *Demineralization*: 2 g of material was added to a solution of 50 mL of HCl (0.25 mol·L^{-1}) in a Becker bottle, and was stirred magnetically (150 rpm, at 50 °C for 2 h). The material was then filtered and washed with distilled water until pH 7 was reached. Finally, the biomaterial obtained after demineralization was dried in an oven (50 °C) for 24 h.

(c) *Deproteinization*: 3g of the material was added to a solution of 50 mL of NaOH (1% *m/v*) in a Becker bottle and kept under constant agitation with a magnetic bar at 80 °C for 3 h. After this, the material was filtered and washed with distilled water until pH 7 was reached. The biomaterial obtained after deproteinization was dried in an oven at 50 °C for 24 h.

(d) *Depigmentation*: For the process of depigmentation and deodorization, 50 mL of sodium hypochlorite solution was added (1% *v/v*) to the biomaterial (236 mg) in a Becker bottle. The material was mechanically agitated on a magnetic stirrer for 8 h at room temperature. It was then filtered and washed until pH 7 was reached. In addition, the filtered material was dried in an oven at 50 °C for 24 h. The biomaterial yield obtained was determined by gravimetric methods.

3.5. Modification of Chitin by Oxone® (CT-Ox)

The modification of the chitin by Oxone® was carried out in a Becker bottle (50 mL), in which 0.5 g of chitin was added to 50 mL of EtOH with 0.5 g of Oxone®. The mixture was placed on a magnetic stirrer for 3 h at 50 °C. After this time, the material was washed with distilled water and dried in an oven (70 °C, for 24 h).

3.6. Optimization Synthesis of Benzylidene Malononitrile 2a Using Biopolymers as Catalysts under Conventional Heating

In a 25 mL round-bottomed flask, the benzylidene malononitrile **2a** was prepared via Knoevenagel condensation reaction using a mixture of benzaldehyde **1a** (2 mmol) and malononitrile (2.5 mmol) and 20% (*w/w* of the malononitrile) of respective biopolymer, both with and without Oxone® [silk fibroin (SF), silk-fibroin-Oxone® (SF-Ox), chitin (CT), and chitin-Oxone® (CT-Ox)] support. A total of 5 mL of water and ethanol mixture (1:1) was used as a solvent and the solution was stirred magnetically for 1–24 h, at a temperature of from 25–50 °C. The catalyst loading was 20% *w/w* of the malononitrile for all the experiments. At the end of the reaction, the precipitate obtained was extracted with EtOAc (3 × 10 mL). The combined organic phases were concentrated by vacuum using a rotary evaporator until total evaporation of the solvent and the residue was purified by washing with hot hexane.

3.7. Synthesis of Benzylidene Malononitrile Derivatives **2a–l** *Using Biopolymers as Catalysts under Conventional Heating*

In a 25 mL round-bottomed flask, the benzylidene malononitrile products **2a–l** were prepared via Knoevenagel condensation reaction from a mixture of appropriate aldehydes **1a–l** (2 mmol), malononitrile (2.5 mmol) and 20% (*w/w* of the malononitrile) of the respective biopolymer with and without Oxone® [silk fibroin (SF), silk-fibroin-Oxone® (SF-Ox), chitin (CT), and chitin-Oxone® (CT-Ox)] support. A total of 5 mL of water and ethanol mixture (1:1) was used as a solvent and the solution was stirred magnetically for 1 h at 50 °C. At the end of the reaction, the precipitate obtained was extracted with EtOAc (3 × 10 mL). The reaction was monitored by TLC. The combined organic phases were vacuum concentrated using a rotary evaporator until total evaporation of the solvent, and the residue obtained was purified by washing with hot hexane. The adducts **2a–l** were characterized by NMR, FTIR, and GC-MS analyses. The spectral data of the compounds were compared with the literature (Supplementary Materials).

3.8. Synthesis of Benzylidene Malononitrile Derivatives **2a–l** *Using Biopolymers as Catalysts under Microwave Irradiation*

In a 25 mL round-bottomed flask, the benzylidene malononitrile products **2a–l** were prepared via Knoevenagel condensation reaction from a mixture of appropriate aldehydes 1a–l (1 mmol), malononitrile (1.25 mmol) and 20% (*w/w* of the malononitrile) of respective biopolymer with supported Oxone® [silk-fibroin-Oxone® (SF-Ox), chitin-Oxone® (CT-Ox)]. A total of 4 mL of water and ethanol mixture (1:1) was used as a solvent and the recipient was put in the microwave reactor and stirred magnetically for 5 min, at 50 °C and at 50 W power. The reaction was monitored by TLC. At the end of the reaction, the precipitate was extracted with EtOAc (3 × 10 mL). The combined organic phases were vacuum concentrated using a rotary evaporator until the total evaporation of the solvent, and the residue obtained was purified by washing with hot hexane. The adducts **2a–l** were characterized by NMR, FTIR, and GC-MS analyses. The spectral data of the compounds were compared with the literature (Supplementary Materials).

3.9. Equipment

The GC-MS analyses were performed on a Shimadzu GC2010plus (Shimadzu®, Kyoto, Japan) coupled to a mass selective detector (Shimadzu MS2010plus) in electron ionization (EI, 70 eV) mode. Analyses were performed with a DB5 column (30 m × 0.25 mm × 0.25 μm, J&W Scientific). The initial oven temperature was 90 °C for 4 min, which was increased to 280 °C at 10 °C min^{-1} and held for 5 min, and finally increased to 300 °C at 10 °C min^{-1} and held for 10 min. The total analysis time was 40 min. The temperatures of the injector and interface were maintained at 250 °C and 270 °C, respectively. Helium was used as a carrier gas with an initial flow of 0.75 mL min^{-1}, and the injection volume was 1 μL (split ratio of 1:20). The ion fragments were detected in the range of 40–550 *m/z*.

FT-IR spectra were recorded on a Shimadzu IRAffinity spectrometer (Shimadzu®, Kyoto, Japan). The samples were prepared on KBr disks and were analyzed in the 4000–400 cm^{-1} region.

NMR spectra were recorded on an Agilent Technologies 500/54 Premium Shielded or Agilent Technologies 400/54 Premium Shielded spectrometer (Agilent Headquarters, Santa Clara, United States), with CD_3OD, DMSO-d_6, or $CDCl_3$ as solvents and TMS as the internal standard. The chemical shifts were given in ppm and the coupling constants (*J*) values were reported in Hz. The deuterated solvents used were $CDCl_3$ (δ_H 7.26, δ_C 77.2); DMSO-d_6 (δ_H 2.50, δ_C 39.5); and CD_3OD (δ_H 4.87, 3.31, δ_C 49.0).

The reactions were performed using a Discover System from CEM Corporation (CEM Corporation, Matthews, NC, USA) at a 2.45 GHz frequency with a maximal power output of 200 W. The power used in the experiments was 50 W.

3.10. Characterization of SF, SF-Ox, CT and CT-Ox

The morphologies of silk fibroin (SF), silk fibroin-Oxone® (SF-Ox), chitin (CT), and chitin-Oxone® (CT-Ox) were observed using scanning electron microscopy (SEM-3030, Hitachi, Tokyo, Japan) at 20 kV.

The FT-IR spectra of the samples (SF, SF-Ox, CT, and CT-Ox) were recorded on a Shimadzu IRAffinity spectrometer. The samples were prepared on KBr disks and were analyzed in the 4000–400 cm^{-1} region.

The thermogravimetric (TG) curves of the samples (SF, SF-Ox, CT, and CT-Ox) were obtained in a TGA-50 thermal analyzer (Shimadzu®, Kyoto, Japan) using a platinum crucible with approximately 5.0 mg of the sample, under a nitrogen atmosphere (N_2) and 50 mL/min flow. The experiment was carried out from room temperature to 600 °C and with a heating rate of 10 °C/min. The data obtained were analyzed using the TA-50W Shimadzu® software package.

4. Conclusions

The present study investigated the use of new materials from natural biopolymers such as fibroin and chitin functionalized with Oxone® (CT-Ox and FS-Ox) in a Knoevenagel condensation reaction using conventional and microwave irradiation as heating sources to synthesize 2-benzylidenemalononitriles **2a–l** under eco-friendly conditions. The biomaterials have the advantage of being biodegradable, easy to obtain, low cost, and compatible with green solvents such as water and ethanol.

Under CH conditions, the biocatalysts exhibited good efficiency for the synthesis of Knoevenagel adducts **2a–l** in reactions performed for 1 h (CT-Ox 71–96% and FS-Ox 60–98%). With the use of MW as a heating source, the reaction time was reduced twelvefold. Compounds **2a–l** were obtained at yields of 39–99% and 35–99% yields CT-Ox and FS-Ox, respectively.

The reuse of biocatalysts was also evaluated. Under CH conditions, CT-Ox was reused for three cycles cycles and a loss of efficiency was observed. SF-Ox, meanwhile, was reused for three cycles without significant efficiency losses. Under MW conditions, CT-Ox could be reused in up to three reaction cycles without any loss of efficiency, while SF-Ox could be used only once, with no loss of catalytic efficiency, but a high loss of mass in the recovery process. However, more studies will be needed to evaluate its catalytic efficiency without significant loss of mass in the recovery process and its applicability in other reactions.

Supplementary Materials: The following supporting information can be downloaded at: https://www.mdpi.com/article/10.3390/catal12080904/s1, Figure S1: ^{1}H NMR (400 MHz, CDCl$_3$) of 2-benzylidenemalononitrile **2a**, Figure S2: ^{13}C NMR (100 MHz, CDCl$_3$) of 2-benzylidenemalononitrile **2a**, Figure S3: FT-IR of 2-benzylidenemalononitrile **2a**, Figure S4: MS (70 eV) of 2-benzylidenemalononitrile **2a**, Figure S5: ^{1}H NMR (500 MHz, CDCl$_3$) of 2-(4-methylbenzylidene)malononitrile **2b**, Figure S6: ^{13}C NMR (125 MHz, CDCl$_3$) of 2-(4-methylbenzylidene)malononitrile **2b**, Figure S7: FT-IR of 2-(4-methylbenzylidene)malononitrile **2b**, Figure S8: MS (70 eV) of 2-(4-methylbenzylidene)malononitrile **2b**, Figure S9: ^{1}H NMR (400 MHz, CDCl$_3$) of 2-(4-(dimethylamino)benzylidene) malononitrile **2c**, Figure S10: ^{13}C NMR (100 MHz, CDCl$_3$) of 2-(4-(dimethylamino)benzylidene)malononitrile **2c**, Figure S11: FT-IR of 2-(4-(dimethylamino)benzylidene)malononitrile **2c**, Figure S12: MS (70 eV) of 2-(4-(dimethylamino)benzylidene)malononitrile **2c**, Figure S13: ^{1}H NMR (500 MHz, CDCl$_3$) of 2-(3,4,5-trimethoxybenzylidene)malononitrile **2d**, Figure S14: ^{13}C NMR (125 MHz, CDCl$_3$) of 2-(3,4,5-trimethoxybenzylidene)malononitrile **2d**, Figure S15: FT-IR of 2-(3,4,5-trimethoxybenzylidene)malononitrile **2d**, Figure S16: MS (70 eV) of 2-(3,4,5-trimethoxybenzylidene)malononitrile **2d**, Figure S17: ^{1}H NMR (400 MHz, MeOD) of 2-(4-hydroxy-3-methoxybenzylidene)malononitrile **2e**, Figure S18: ^{13}C NMR (100 MHz, MeOD) of 2-(4-hydroxy-3-methoxybenzylidene)malononitrile **2e**, Figure S19: FT-IR of 2-(4-hydroxy-3-methoxybenzylidene)malononitrile **2e**, Figure S20: MS (70 eV) of 2-(4-hydroxy-3-methoxybenzylidene)malononitrile **2e**, Figure S21: ^{1}H NMR (400 MHz, CDCl$_3$) of 2-(4-fluorobenzylidene)malononitrile **2f**, Figure S22: ^{13}C NMR (100 MHz, CDCl$_3$) of 2-(4-fluorobenzylidene)malononitrile **2f**, Figure S23: FT-IR of 2-(4-fluorobenzylidene)malononitrile **2f**, Figure S24: MS (70 eV) of 2-(4-fluorobenzylidene)malononitrile **2f**, Figure S25: ^{1}H NMR (500 MHz, CDCl$_3$) of 2-(4-

chlorobenzylidene)malononitrile **2g**, Figure S26: ^{13}C NMR (125 MHz, CDCl$_3$) of 2-(4-chlorobenzyliden e)malononitrile **2g**, Figure S27: FT-IR of 2-(4-chlorobenzylidene)malononitrile **2g**, Figure S28: MS (70 eV) of 2-(4-chlorobenzylidene)malononitrile **2g**, Figure S29: ^{1}H NMR (400 MHz, CDCl$_3$) of 2-(4-bromobenzylidene)malononitrile **2h**, Figure S30: ^{13}C NMR (100 MHz, CDCl$_3$) of 2-(4-bromobenzylide ne)malononitrile **2h**, Figure S31: FT-IR of 2-(4-bromobenzylidene)malononitrile **2h**, Figure S32: MS (70 eV) of 2-(4-bromobenzylidene)malononitrile **2h**, Figure S33: ^{1}H NMR (500 MHz, CDCl$_3$) of 2-(4-hydroxybenzylidene)malononitrile **2i**, Figure S34: ^{13}C NMR (125 MHz, CDCl$_3$) of 2-(4-hydroxybenzylidene)malononitrile **2i**, Figure S35: FT-IR of 2-(4-hydroxybenzylidene)malononitrile **2i**, Figure S36: MS (70 eV) of 2-(4-hydroxybenzylidene)malononitrile **2i**, Figure S37: ^{1}H NMR (500 MHz, CDCl$_3$) of 2-(4-nitrobenzylidene)malononitrile **2j**, Figure S38: ^{13}C NMR (125 MHz, CDCl$_3$) of 2-(4-nitrobenzylidene)malononitrile **2j**, Figure S39: FT-IR of 2-(4-nitrobenzylidene)malononitrile **2j**, Figure S40: MS (70 eV) of 2-(4-nitrobenzylidene)malononitrile **2j**, Figure S41: ^{1}H NMR (400 MHz, CDCl$_3$) of 2-(4-cyanobenzylidene)malononitrile **2k**, Figure S42: ^{13}C NMR (100 MHz, CDCl$_3$) of 2-(4-cyanobenzylidene)malononitrile **2k**, Figure S43: FT-IR of 2-(4-cyanobenzylidene)malononitrile **2k**, Figure S44: MS (70 eV) of 2-(4-cyanobenzylidene)malononitrile **2k**, Figure S45: ^{1}H NMR (400 MHz, CDCl$_3$) of (2-methyl-3-phenylallylidene)malononitrile **2l**, Figure S46: ^{13}C NMR (100 MHz, CDCl$_3$) of (2-methyl-3-phenylallylidene)malononitrile **2l**, Figure S47: FT-IR of 2-(3-phenylallylidene)malononitri le **2l**, Figure S48: MS (70 eV) of 2-(3-phenylallylidene)malononitrile **2l**.

Author Contributions: Conceptualization, F.B.N., S.A.Y., D.E.Q.J. and I.M.F.; methodology, F.B.N., L.L.Z., R.M.R.C., A.N.d.O. and R.R.P.; formal analysis, J.O.C.S.J., R.M.R.C., L.L.Z. and D.E.Q.J.; investigation, F.B.N., A.L.M.P., S.A.Y. and I.M.F.; resources, A.N.d.O. and D.E.Q.J.; data curation, I.M.F.; writing—original draft preparation, A.L.M.P., S.A.Y. and I.M.F.; writing—review and editing, J.O.C.S.J., R.M.R.C., L.L.Z., D.E.Q.J., I.M.F., S.A.Y. and A.L.M.P.; visualization, F.B.N., L.L.Z., D.E.Q.J., A.N.d.O. and R.R.P.; project administration, I.M.F.; funding acquisition, I.M.F., S.A.Y. and A.L.M.P. All authors have read and agreed to the published version of the manuscript.

Data Availability Statement: All data is provided in full in the results section of this paper.

Conflicts of Interest: The authors declare no conflict of interest.

References

1. Jimenez, D.E.Q.; Zanin, L.L.; Diniz, L.F.; Ellena, J.; Porto, A.L.M. Green Synthetic Methodology of (*E*)-2-cyano-3-aryl Selective Knoevenagel Adducts Under Microwave Irradiation. *Curr. Microw. Chem.* **2019**, *6*, 54–60. [CrossRef]
2. Chakraborty, S.; Paul, A.R.; Majumdar, S. Base and metal free true recyclable medium for Knoevenagel condensation reaction in SDS-ionic liquid-aqueous miceller composite system. *Results Chem.* **2022**, *4*, 100294. [CrossRef]
3. Bi, S.; Meng, F.; Wu, D.; Zhang, F. Synthesis of vinylene-linked covalent organic frameworks by monomer Self-catalyzed activation of Knoevenagel condensation. *J. Am. Chem. Soc.* **2022**, *8*, 3653–3659. [CrossRef] [PubMed]
4. Tran, V.A.; Quynh, L.T.N.; Vo, T.T.; Nguyen, P.A.; Don, T.N.; Vasseghian, Y.; Phan, H.; Lee, S.W. Experimental and computational investigation of a green Knoevenagel condensation catalyzed by zeolitic imidazolate framework-8. *Environ. Res.* **2022**, *204*, 112364–112374. [CrossRef] [PubMed]
5. Kalla, R.M.N.; Park, H.; Lee, H.R.; Suh, H.; Kim, I. Efficient, Solvent-Free, Multicomponent Method for Organic-Base-Catalyzed Synthesis of β-Phosphonomalonates. *ACS Comb. Sci.* **2015**, *17*, 691–697. [CrossRef] [PubMed]
6. Birolli, W.G.; Zanin, L.L.; Jimenez, D.E.Q.; Porto, A.L.M. Synthesis of Knoevenagel Adducts Under Microwave Irradiation and Biocatalytic Ene-Reduction by the Marine-Derived Fungus *Cladosporium* sp. CBMAI 1237 for the Production of 2-Cyano-3-Phenylpropanamide Derivatives. *Mar. Biotechnol.* **2020**, *22*, 317–330. [CrossRef] [PubMed]
7. Lv, H.; Zhang, Z.; Fan, L.; Gao, Y.; Zhang, X. A nanocaged cadmium-organic framework with high catalytic activity on the chemical fixation of CO$_2$ and deacetalization-knoevenagel condensation. *Microporous Mesoporous Mater.* **2022**, *335*, 111791–111800. [CrossRef]
8. Yang, X.; Fox, T.; Berke, H. Facile metal free regioselective transfer hydrogenation of polarized olefins with ammonia borane. *Chem. Commun.* **2011**, *47*, 2053–2055. [CrossRef] [PubMed]
9. Ferreira, I.M.; Yoshioka, S.A.; Comasseto, J.V.; Porto, A.L.M. Immobilization of Amano lipase from *Pseudomonas fluorescens* on silk fibroin spheres: An alternative protocol for the enantioselective synthesis of halohydrins. *RSC Adv.* **2017**, *7*, 12650–12658. [CrossRef]

10. Júnior, E.B.M.; Neves, F.B.; Lopes, S.Q.; Holanda, F.H.; Souza, T.M.; Pinto, E.P.; Oliveira, A.N.; Fonseca, L.P.; Yoshioka, S.A.; Ferreira, I.M. Immobilization of Amano AK Lipase from *Pseudomonas fluorescens* on Novel Silk Microfiber using Oxone®: Parameter Optimization for Enzymatic Assays and use in Esterification of Residual Palm Oil. *Curr. Catal.* **2021**, *10*, 119–129. [CrossRef]

11. Ferreira, I.M.; Ganzeli, L.; Rosset, I.G.; Yoshioka, S.A.; Porto, A.L.M. Ethylic Biodiesel Production Using Lipase Immobilized in Silk Fibroin-Alginate Spheres by Encapsulation. *Catal. Lett.* **2017**, *147*, 269–280. [CrossRef]

12. Kuhbeck, D.; Ghosh, M.; Gupta, S.S.; Díaz, D.D. Investigation of C-C bond formation mediated by *bombyx mori* Silk Fibroin Materials. *ACS Sustain. Chem. Eng.* **2014**, *2*, 1510–1517. [CrossRef]

13. Knidri, H.E.L.; Dahmani, J.; Addaou, A.; Laajeb, A.; Lahsini, A. Rapid and efficient extraction of chitin and chitosan for scale-up production: Effect of process parameters on deacetylation degree and molecular weight. *Int. J. Biol. Macromol.* **2019**, *139*, 1092–1102. [CrossRef]

14. Madkour, M.; Khalil, K.D.; Al-Sagheer, F.A. Heterogeneous Hybrid Nanocomposite Based on Chitosan/Magnesia Hybrid Films: Ecofriendly and Recyclable Solid Catalysts for Organic Reactions. *Polymers* **2021**, *13*, 3583. [CrossRef]

15. Moussout, H.; Ahlafi, H.; Aazza, M.; Bourakhouadar, M. Kinetics and mechanism of the thermal degradation of biopolymers chitin and chitosan using thermogravimetric analysis. *Polym. Degrad. Stab.* **2016**, *130*, 1–9. [CrossRef]

16. Rani, D.; Singla, P.; Agarwal, J. 'Chitosan in water' as an eco-friendly and efficient catalytic system for Knoevenagel condensation reaction. *Carbohydr. Polym.* **2018**, *202*, 355–364. [CrossRef] [PubMed]

17. Hirayama, Y.; Kanomata, K.; Hatakeyama, M.; Kitaoka, T. Chitosan nanofiber-catalyzed highly selective Knoevenagel condensation in aqueous methanol. *RSC Adv.* **2020**, *10*, 26771–26776. [CrossRef] [PubMed]

18. Abrantes, P.G.; Costa, I.F.; Falcão, N.K.S.M.; Ferreira, J.M.G.O.; Junior, C.G.L.; Teotonio, E.E.S.; Vale, J.A. The Efficient Knoevenagel Condensation Promoted by Bifunctional Heterogenized Catalyst Based Chitosan-EDTA at Room Temperature. *Catal. Lett.* **2022**, *1*, 1–11. [CrossRef]

19. Trotzki, R.; Hoffmann, M.M.; Ondruschka, B. The knoevenagel condensation at room temperature. *Green Chem.* **2008**, *10*, 873–887. [CrossRef]

20. Anbu, N.; Hariharan, S.; Dhakshinamoorthy, A. Knoevenagel-Doebner condensation promoted by chitosan as a reusable solid base catalyst. *Mol. Catal.* **2020**, *484*, 110744. [CrossRef]

21. Luong, J.H.T.; Gedanken, A. Eco-Friendly and Facile Preparation of Spherical Chitin Nanoparticles. *ChemistrySelect* **2018**, *3*, 10787–10791. [CrossRef]

22. Lopes, S.Q.; Holanda, F.H.; Jimenez, D.E.Q.; Nascimento, L.A.S.; Oliveira, A.N.; Ferreira, I.M. Use of Oxone® as a Potential Catalyst in Biodiesel Production from Palm Fatty Acid Distillate (PFAD). *Catal. Lett.* **2021**, *10*, 24–26. [CrossRef]

23. Perin, G.; Santoni, P.; Barcellos, A.M.; Nobre, P.C.; Jacob, R.G.; Lenardão, E.J.; Santi, C. Selenomethoxylation of Alkenes Promoted by Oxone®. *Eur. J. Org. Chem.* **2018**, *2018*, 1224–1229. [CrossRef]

24. Kumar, S.; Foroozesh, J. Chitin nanocrystals based complex fluids: A green nanotechnology. *Carbohydr. Polym.* **2021**, *257*, 117619. [CrossRef] [PubMed]

25. Devadiga, A.; Vidya Shetty, K.; Saidutta, M.B. Highly stable silver nanoparticles synthesized using *Terminalia catappa* leaves as antibacterial agent and colorimetric mercury sensor. *Mater. Lett.* **2017**, *207*, 66–71. [CrossRef]

26. Drnovšek, N.; Kocen, R.; Gantar, A.; Drobnič-Košorok, M.; Leonardi, A.; Križaj, I.; Rečnik, A.; Novak, S. Size of silk fibroin β-sheet domains affected by Ca²⁺. *J. Mater. Chem. B* **2016**, *4*, 6597–6608. [CrossRef]

27. Rwegasila, E.; Mubofu, E.B.; Nyandoro, S.S.; Erasto, P.; Munissi, J.J.E. Preparation, characterization and in vivo antimycobacterial studies of panchovillin-chitosan nanocomposites. *Int. J. Mol. Sci.* **2016**, *17*, 1559. [CrossRef] [PubMed]

28. Mohan, K.; Muralisankar, T.; Jayakumar, R.; Rajeevgandhi, C. A study on structural comparisons of α-chitin extracted from marine crustacean shell waste. *Carbohydr. Polym. Technol. Appl.* **2021**, *2*, 100037. [CrossRef]

29. Barbosa, H.F.G.; Francisco, D.S.; Ferreira, A.P.G.; Cavalheiro, É.T.G. A new look towards the thermal decomposition of chitins and chitosans with different degrees of deacetylation by coupled TG-FTIR. *Carbohydr. Polym.* **2019**, *225*, 115232. [CrossRef] [PubMed]

30. Nogueira, G.M.; Rodas, A.C.D.; Leite, C.A.P.; Giles, C.; Higa, O.Z.; Polakiewicz, B.; Beppu, M.M. Preparation and characterization of ethanol-treated silk fibroin dense membranes for biomaterials application using waste silk fibers as raw material. *Bioresour. Technol.* **2010**, *101*, 8446–8451. [CrossRef] [PubMed]

31. Assis, O.B.G.; de Britto, D.; Forato, L.A. O Uso de Biopolímeros como Revestimentos Comestíveis Protetores Para Conservação de Frutas in natura e minimamente processadas. *Boletim de Pesquisa e Desenvolvimento* **2009**, *29*, 1–24.